

UDC 621.3:681.34

R.A. KOZHEMIKIN¹, S.S. KRIVENKO¹, V.V. LUKIN¹, R.C.P. MARQUES²,
F.N.S. DE MEDEIROS², B. VOZEL³

¹ *Dept of Transmitters, Receivers and Signal Processing National Aerospace University, Kharkov, Ukraine*

² *Teleinformatics Dept, Federal University of Ceara DETI-UFC Fortaleza CE, Brazil*

³ *University of Rennes 1, CS 80518, 22305, Lannion Cedex, France*

EFFICIENCY ANALYSIS OF COMBINED DESPECKLING OF SINGLE-LOOK SAR IMAGES

Efficiency of Synthetic Aperture Radar (SAR) image despeckling is assessed using model data that take into account basic properties of real-life single-look images, in particular non-Gaussian probability density function of fully-developed speckle and its spatial correlation. Analysis is performed for a wide set of well-known despeckling techniques and for recently proposed locally adaptive filters that combine a Level Set method used to detect small-sized objects and Discrete Cosine transform based denoising. The despeckling performance is evaluated in terms of standard criterion (output MSE) and two other criteria – local MSE in heterogeneous regions and integral MSSIM. The experiments have demonstrated that the locally adaptive filters outperform the well-known ones.

Key words: *single-look SAR image; combined despeckling; Level Set method, DCT, efficiency analysis.*

Introduction

Synthetic aperture radars have become a standard imaging tool installed on-board of airborne and spaceborne carriers [1, 2]. The main advantage of SAR (Synthetic Aperture Radar) systems is their ability to acquire data in different weather conditions, during day and night, and with high spatial resolution. However, high resolution can be provided if a SAR sensor operates in single-look mode for which acquired images are characterized by the presence of a noise-like phenomenon also called speckle [1, 3].

Speckle can be treated as a special kind of multiplicative noise that has several peculiarities. First, its probability density function (PDF) is not Gaussian for single-look and multi-look modes (if the number of looks is not too large [1, 4]). Second, the spatial correlation of the speckle is often observed for real-life SAR images [5, 6], which is usually ignored in image modeling and at the stage of SAR data processing [1, 4-7]. By data processing, we mean here such operations as edge and target detection as well as SAR image pre-filtering. Note that SAR image pre-filtering (often called despeckling) is a standard operation in dealing with SAR data [1, 3-9]. It allows more accurate estimation of radar cross-section in homogeneous regions, provides easier segmentation, ensures more reliable solving classification tasks, simplifies visual analysis of SAR images by human experts [1, 3, 10], etc.

Numerous techniques for SAR image despeckling

have been already proposed (see [3-7, 9-12] and references therein). These techniques are based on different principles including scanning window filtering, orthogonal transforms, total variation, non-local approaches, etc. Most of these methods provide rather efficient speckle suppression in homogeneous image regions and quite good preservation of edges. Most of them are also able to preserve texture features and small-sized objects to some extent although texture/detail preservation is still worth improving.

One problem in designing new techniques for SAR image despeckling as well as the performance assessment for them is the absence of commonly accepted test (noise-free) and simulated (noisy) SAR images. A similar problem was actual for researchers dealing with optical image processing. They solved it by accepting a standard set of grayscale and color images that includes benchmark images (e.g. Lena, Baboon, Barbara, Peppers, etc.). Meanwhile, SAR image processing community still adopts the following three practices. The first practice simulates speckle for standard optical images as Lena, Boats, etc. [11, 13]. The second one generates speckled images on the basis of optical images of natural scenes acquired from airborne platforms [11]. Finally, the third practice applies and analyses real-life images before and after despeckling [11, 14].

The first practice provides quantitative evaluation of the filtering efficiency although speckle spatial correlation is often ignored in this case. Besides, this

approach has been criticized in the sense that noise-free optical characteristics and true SAR images are different. From this viewpoint, the second practice provides more adequate properties of noise-free and speckled images. Some typical effects in SAR data as, e.g., shadowing can not be still represented and, thus, taken into account. A drawback of the third practice is that it allows to calculate only particular parameters characterizing filtering efficiency as, e.g., increase of equivalent number of looks (ENL). However, estimates of such parameters can be not accurate enough and edge/detail/texture preservation is analyzed mostly visually, i.e., subjectively.

These shortcomings have stimulated the design of more sophisticated SAR image models [12, 15, 16]. They are able to simulate spatially correlated speckle [15] and other more complex phenomena in single- and multi-look SAR images [12, 16].

The goal of this paper is to carry out quantitative performance analysis and comparison for a wide set of modern despeckling techniques. Peculiarities of our study consist in using more adequate models of single-look SAR images that take into account spatial correlation of the noise as well as in exploiting three quantitative criteria, namely, integral output mean squared error (MSE) calculated for entire image, local MSE determined for locally active areas of the test images, and the metric MSSIM [17] that is able to adequately characterize visual quality of original (noisy) and despeckled images. Whilst the first quantitative criterion is traditional, the two latter ones are less often used in analysis. Meanwhile, both are important since heterogeneities and visual quality are of great importance in SAR image processing [1, 18]. One more peculiarity is that heterogeneity areas are detected using the Level Set approach [19] that has recently demonstrated its effectiveness in processing SAR and other types of noisy images [14, 20-23].

2. Model test images and criteria of filtering efficiency

This paper focuses on filtering single-look SAR images. This is the most complex and challenging case because of the highest intensity of the speckle. There are two possibilities to model noisy test SAR images. In both cases, the noisy model is expressed as [1]:

$$I_{ij}^n = I_{ij}^{\text{true}} \mu_{ij}, \quad (1)$$

where I_{ij}^{true} stands for the true image value in ij -th pixel and μ_{ij} is the multiplicative noise with unitary mean. In the first case, one considers amplitude data for which

speckle variance $\sigma_{\mu}^2 = 0.273$ and follows a Rayleigh distribution. In the second case, intensity images are considered where PDF is negative exponential and $\sigma_{\mu}^2 = 1.0$. In our paper, without losing generality, we study the former case (original and filtered images for the two cases can be easily converted from one to another representation by simple homomorphic transforms [1]).

A specific feature of the model (1) in our study is that speckle is modeled as spatially correlated multiplicative noise. Spatial correlation properties of the speckle are modeled in such a way that they are practically the same as for single-look SAR images produced by TerraSAR-X spaceborne sensor [24]. The simulation algorithm is presented in [25]. The noise-free test image # 1 is presented in Fig. 1.a whilst the obtained noisy version is shown in Fig. 1.b. Noise-free test images are in 8-bit bitmap format whilst noisy images are represented as 16-bit 2D data arrays to avoid clipping effects. Filtered images have been presented in the latter format as well to diminish the influence of rounding-off errors on estimates of filtering efficiency criteria.

Output (integral) MSE is calculated as

$$\text{MSE}_{\text{out}} = \sum_{i=1}^{I_{\text{IM}}} \sum_{j=1}^{J_{\text{IM}}} (I_{ij}^f - I_{ij}^{\text{true}})^2 / (I_{\text{IM}} J_{\text{IM}} - 1), \quad (2)$$

where I_{ij}^f stands for a filtered image value in ij -th pixel, I_{IM} and J_{IM} define the image size (both considered test images are of size 512x512 pixels).

In addition to the traditional output MSE, local MSE MSE_{het} has been determined for heterogeneous image regions as

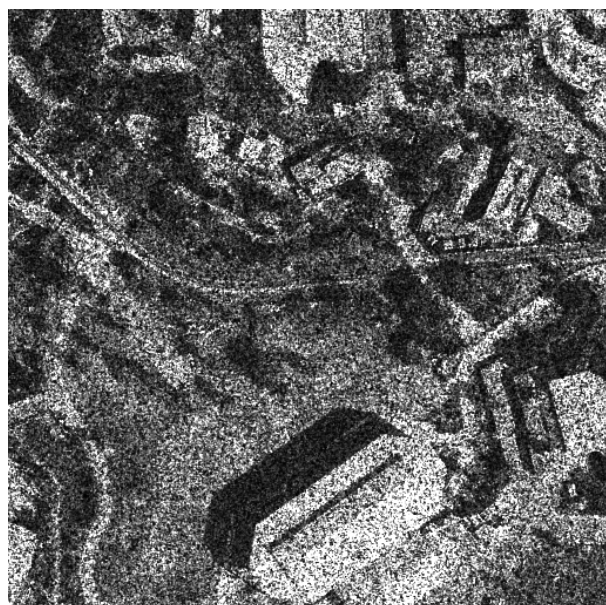
$$\text{MSE}_{\text{out}} = \sum_{i,j \in G_{\text{het}}} (I_{ij}^f - I_{ij}^{\text{true}})^2 / (|N_{G_{\text{het}}}| - 1), \quad (3)$$

where G_{het} denotes a set of pixels that belong to heterogeneous regions, $N_{G_{\text{het}}}$ is the number of pixels in this set.

These heterogeneous regions have been detected using the Level Set method that locates small-sized objects and delimits their boundaries. This approach is based on the Hamilton-Jacobi equation [22, 23]. Its ability to detect heterogeneities in single-look SAR images has been studied for simulated and real-life data in [14]. After detecting region contours, we perform a post-processing to produce a binary map. Fig. 2.a illustrates an example of this map for the test image # 1 (Fig. 1). In fact, small-sized objects, edges and their neighborhoods are detected well.



a



b

Fig. 1. A test noise-free image #1 (a) and the corresponding noisy image (b)

The third considered metric is MSSIM [17] determined for the entire test image. The reasons for using it are that it is one of the best visual quality metrics for grayscale images [26], since it takes into account several valuable aspects of human visual system. Moreover, the MSSIM metric encompasses the Weber-Fechner law that describes different sensitivity of humans to distortions in image fragments with different local mean (brightness). Thus, in this paper this is a relevant aspect for the speckle noise.

Speckle filtering was first introduced over 30 years ago and, since then, filtering methods as the local statistic Lee and Frost filters [7, 27, 28] have undergone a continuous refinement. The obtained data are presented in Table 1 for both test images. As it is known, the performance of these filters depends on the scanning window size. Thus, we applied several window sizes in order to determine the optimal one according to the used criteria. The refined Lee filter implementation available at [http://www.mathworks.com/matlabcentral/fileexchange/9456-lee-filter] has been used. It is worth noting that better efficiency of noise suppression in homogeneous regions for both filters is provided by larger scanning window sizes. According to the data analysis, the optimal scanning window size for the Lee filter is 7×7 pixels usually recommended for practical application.

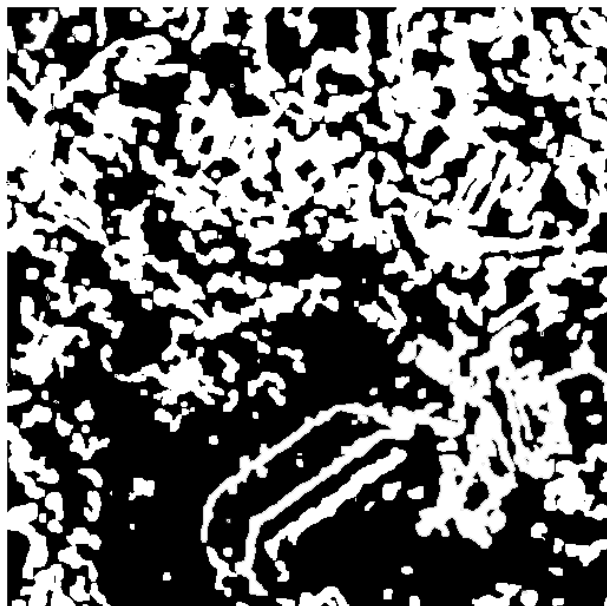
Meanwhile, scanning window size of 5×5 pixels provides better edge and detail preservation. Concerning the Frost filter, a 17×17 scanning window achieves the smallest (the best) output MSE whilst the best visual quality is accomplished by a 13×13 pixel scanning window. Finally, the smallest MSE_{het} is observed for 9×9 scanning window size. In general, the results for the Frost filter (e.g., with the scanning window 13×13 pixels) are sufficiently better than for the local statistic Lee filter. Moreover, the Frost filter performs superior when compared to other, more sophisticated, filters as it will be seen from further analysis.

Table 1
Performance of the local statistic Lee and Frost filters

Scanning window size	Test image # 1			Test image # 2		
	MSE out	MSE het	MSSIM	MSE out	MSE het	MSSIM
Lee 5×5	620	783	0.778	640	831	0.766
Lee 7×7	567	843	0.780	598	988	0.767
Lee 9×9	589	958	0.761	625	1176	0.747
Frost 5×5	630	729	0.777	643	712	0.764
Frost 9×9	479	663	0.810	503	703	0.799
Frost 13×13	460	670	0.817	485	722	0.806
Frost 17×17	459	677	0.816	484	734	0.805

Another denoising technique used for comparison is the integro-differential filter [29]. Actually, this filter also depends on the scanning window size and the results for windows from 5×5 to 15×15 are presented (denoted as Vozel 5, ..., Vozel 15). The obtained data are presented in Table 2. As it can be seen, the minimal local MSE was observed for 7×7 scanning window whilst

optimal integral MSE and the best visual quality was provided for 9x9 scanning window.



a



b

Fig. 2. Heterogeneity detection map (a) and the noise-free test image # 2 (b)

Table 2 also displays data for the BM3D (block matching 3-dimensional) filter [30] equipped by the corresponding variance stabilizing transformations (VST) [13]. This denoising technique has provided the output MSE and local MSE sufficiently larger than for the Frost filter with optimal parameters, and the MSSIM metric achieved the worse value. Note that the BM3D filter is considered to be the state-of-the-art nowadays in

suppressing additive white Gaussian noise. Possible reasons why it has not performed well enough for the considered application are the following. First, the noise in images after direct homomorphic (variance stabilizing) transform is not white and not Gaussian [1]. This makes the task of similar patch search more complicated [31]. Second, the found similar patches are processed by the DCT based denoising not adapted to spatial spectrum of the noise. This additionally makes performance of the denoising worse. Then, it can be expected that performance of the BM3D based filtering can be improved if these drawbacks are undertaken and the corresponding modifications are employed.

The Level set based despeckling method encompasses a target detection algorithm that adopts a measure of homogeneity/heterogeneity to discriminate small-sized objects surrounded by large homogeneous areas [23]. Then, the speckle filtering method performs in blocks over homogeneous regions and furthermore preserves edges and details. Table 3 presents the performance assessment of this filtering scheme. In fact, its performance depends on the number of iterations and the higher iterations produce better results in the sense of MSE_{out} and MSE_{het} . However, the obtained results are considerably worse than for the Frost filter and the technique [29] with optimal parameters.

Table 2

The performance of the integro-differential filter and BM3D with VST

Scanning window size	Test image # 1			Test image # 2		
	MSE _{out}	MSE _{het}	MSSIM	MSE _{out}	MSE _{het}	MSSIM
Vozel 3	732	813	0.764	736	763	0.751
Vozel 5	510	651	0.807	526	520	0.795
Vozel 7	452	627	0.821	477	672	0.810
Vozel 9	438	634	0.824	467	692	0.812
Vozel 11	439	652	0.821	469	714	0.809
Vozel 13	446	672	0.816	477	735	0.803
Vozel 15	457	693	0.809	486	754	0.796
BM3D with VST	746	872	0.756	762	809	0.743

Table 3

The performance of the Level Set based despeckling

Number of iterations	Test image # 1			Test image # 2		
	MSE _{out}	MSE _{het}	MSSIM	MSE _{out}	MSE _{het}	MSSIM
1	1521	1519	0.710	1523	1377	0.696
2	952	1087	0.756	974	1101	0.743
3	765	957	0.773	793	1015	0.762
4	694	920	0.777	724	985	0.765
5	668	913	0.773	696	987	0.762

Consider the DCT based filtering. This despeckling approach presents many variants. Here, we specify the

one considered in the proposed approach. We assume the processing of fully overlapping blocks and adapt this filtering process to spatial DCT spectrum of the noise by applying the following combined thresholding [14, 32]:

$$D_t(m, n, k, l) = \begin{cases} D(m, n, k, l), & \text{if } |D(m, n, k, l)| \geq \beta \sigma_\mu I_{mn}^{\text{mean}} \sqrt{W_{kl}}; \\ D^3(m, n, k, l) / (\beta \sigma_\mu I_{mn}^{\text{mean}} \sqrt{W_{kl}})^2 & \text{otherwise,} \end{cases} \quad (4)$$

where $D(m, n, k, l)$ is the kl -th DCT coefficient of the block with left upper corner and indices m and n . Here, I_{mn}^{mean} denotes the mean for the mn -th block, W_{kl} is the normalized DCT spectrum of the speckle, k and l are indices in the DCT domain, β is a parameter which the recommended value is equal to 4.5. A typical block size is 8×8 pixels and furthermore, we evaluate data obtained for each block and several different values of the parameter β . The results are presented in Table 4 and from the analysis of them, we conclude:

- 1) there are minima for both (entire image) output MSE and local MSE (determined for pixels that belong to map);
- 2) these minima are observed for different β , minimal local MSE is observed for smaller β (about 4.6) since smaller β in DCT based filtering provides better preservation of edges and details;
- 3) there are also maximum values for the MSSIM metric (that characterizes visual quality) observed practically for the same β as minimum of the local MSE;
- 4) the best provided criteria values are almost the same as for the Frost filter with the optimal parameter settings and slightly worse than for the filtering technique [29].

Table 4
The performance of the DCT-based despeckling combined with frequency dependent thresholding and 8×8 pixel blocks

β	Test image # 1			Test image # 2		
	MSEout	MSE het	MSSIM	MSEout	MSE het	MSSIM
3.8	547	729	0.810	562	734	0.801
4.0	519	704	0.813	537	715	0.804
4.2	499	688	0.815	518	703	0.806
4.4	485	678	0.816	504	698	0.807
4.6	475	673	0.816	495	698	0.808
4.8	468	672	0.816	489	701	0.807
5.0	464	674	0.816	486	708	0.807
5.2	462	678	0.815	484	717	0.806
5.4	462	684	0.814	484	728	0.805
5.6	463	691	0.813	486	741	0.803

Based on the result analysis presented in [33] for intensive noise, one might expect that better results for the considered application can be provided by the DCT-based filters with 16×16 pixel blocks. To check this hypothesis, we have obtained simulation data for this version of the DCT-based despeckling which are displayed in Table 5. Although the obtained values of the studied criteria are satisfactory, they are worse than those ones presented for the Frost, Vozel's and 8×8 block DCT filters with optimal parameters. The main problem is with edge/detail preservation for image processing in 16×16 blocks.

The studies have been also performed for the hard frequency dependent thresholding with block sizes of 8×8 and 16×16 pixels. The difference between them both is that optimal β values are about 3 according to output MSE (minimum) and about 2.8 according to local MSE minimum and MSSIM maximum.

Table 5
The performance of the DCT-based despeckling combined with frequency dependent thresholding, 16×16 pixel blocks

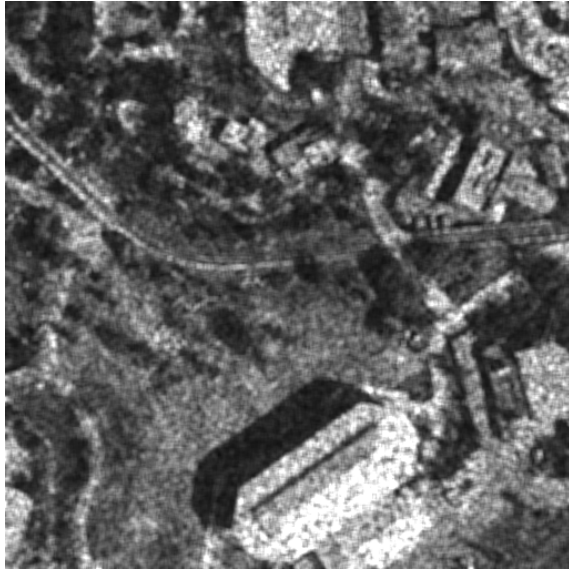
β	Test image # 1			Test image # 2		
	MSEout	MSE het	MSSIM	MSEout	MSE het	MSSIM
4.0	527	721	0.809	547	755	0.798
4.2	510	713	0.809	530	758	0.799
4.4	498	712	0.809	520	766	0.798
4.6	492	717	0.807	515	780	0.796
4.8	489	725	0.805	513	796	0.793
5.0	490	736	0.801	514	816	0.790

It is worth noting that local MSE for all studied despeckling approaches is always larger than output MSE for the entire image. This is due to the fact that any filter better suppresses noise in homogeneous image regions than in heterogeneous ones [27, 28, 34, 35]. Moreover, heterogeneity regions usually correspond to pixel areas with large local mean and, therefore, large local (input) MSE due to multiplicative nature of speckle.

Fig. 3 exemplifies two examples of filtered images. As it can be seen, the DCT-based filter has succeeded in suppressing speckle considerably and provided better edge/detail preservation although it is still worth improving.

4. Performance analysis for combined approaches to despeckling

Summarizing the simulation results presented in the previous section, one can expect that further improvement of despeckling efficiency can be provided due to the better preservation of fine details (targets) and edges, i.e. better processing of single-look SAR



a



b

Fig. 3. Output images (# 1) for the 7x7 refined Lee filter (a) and the DCT based filter (combined frequency dependent thresholding with $\beta = 4.9$) (b)

images in heterogeneous regions. Note that the area that corresponds to such heterogeneous regions is quite large. For the noisy test image in Fig. 1.b, the percentage of such pixels is about 44% in the mappresented in Fig. 2.a (white pixels). We assume that heterogeneous regions can be detected by the Level Set method. Then, the task is to attain the local MSE as small as possible.

Improvement for edge/detail preservation has been earlier proposed in [14] and its efficiency has been demonstrated qualitatively but not quantitatively. Thus, below we focus on the MSE_{het} and $MSSIM$ criteria for

several versions of the combined (locally adaptive) despeckling techniques.

Our assumption is that the 8x8 block DCT-based filter combined with frequency dependent thresholding ($\beta = 4.9$) is proper for processing homogeneous image regions. Thus, we have to check which filter is more suitable to apply to the detected heterogeneous regions.

In [14], it is proposed to apply the DCT-based filtering combined with frequency-independent hard thresholding:

$$D_t(m, n, k, l) = \begin{cases} D(m, n, k, l), & \text{if } |D(m, n, k, l)| \geq \beta \sigma_\mu I_{mn}^{med}; \\ 0, & \text{otherwise,} \end{cases} \quad (5)$$

where I_{mn}^{med} is the median value in mn -th block. In fact, there are two main approaches to exploit. First, adaptation to speckle spatial spectrum is used in homogeneous regions due to (4). Second, adaptation to local content is applied due to detecting heterogeneous areas by the Level Set method and adjusting better edge-detail preservation for these areas.

We have checked this locally adaptive version and the provided results are presented in Table 6. As it can be seen, the obtained values of MSE_{out} , MSE_{het} , and $MSSIM$ are better than for any DCT-based filter studied above for both test images.

The other option was proposed in [14] and applies the 8x8 block Haar wavelet based thresholding in detected heterogeneous areas. We have first analyzed performance of the Haar wavelet denoising itself. It has been established that approximately the same (optimal) results are obtained if the hard threshold is set either as expression $T(m, n) = \beta \sigma_\mu I_{mn}^{mean}$, $\beta \approx 3.5$ or as expression

$T(m, n) = \beta \sigma_\mu I_{mn}^{med}$, $\beta \approx 4.0$. The obtained simulation data for the latter variant are given in Table 6. The results are slightly better than for the first version of adaptive filter.

Since very good results have been provided by the Frost filter, it inspired the idea that DCT-based denoising with frequency-dependent thresholding can be combined with the Frost filter. The corresponding locally adaptive filter output can be expressed as

$$I_{ad}(i, j) = \begin{cases} a_1 I_{DCT}(i, j) + a_2 I_{Fr}(i, j), & \text{if } M(i, j) = 0; \\ a_3 I_{DCT}(i, j) + a_4 I_{Fr}(i, j), & \text{otherwise,} \end{cases} \quad (6)$$

where for non-negative weights $a_1 + a_2 = 1, a_3 + a_4 = 1, a_1 \geq a_3$, $I_{DCT}(i, j), I_{Fr}(i, j)$ are the DCT and Frost filter outputs for an ij -th pixel, $M(i, j) = 0$ denotes local

activity map values for locally passive areas (where heterogeneities are not detected by the Level Set technique). In addition, we employed another mechanism to improve the despeckling scheme here. We assume that the outputs of the two filters are correlated, although the correlation factor is not equal to unity. Then, some partly averaging of residual noise can be provided.

We have studied the combined filtering for 8x8 block DCT with combined thresholding with $\beta \approx 4.9$ and the 9x9 Frost filter. The obtained results ($a_1 = 0.6, a_3 = 0.4$) are presented in the lowest row of Table 6 (denoted as DCT+Frost). Although there is some improvement compared to the basic DCT and Frost filters, the benefit is not sufficient. The reason is that residual noise is highly correlated for these filters.

Similarly to (6), we have combined the DCT-based denoising with the filter introduced in [29]. The only difference is that in this case $a_1 = a_2 = 0.5, a_3 = 0.3, a_4 = 0.7$. The results are presented in the lowest row of Table 6. In general, these results are better than for any other considered denoising method considered in this study.

heterogeneous regions. First, we have used $\beta=4.0$ according to Table 6. The output image is presented in Fig. 4.a and we observe edge-detail preservation compared to the non-adaptive variant (see output image in Fig. 3.b). One can expect that edge sharpness can be even better if β is smaller than 4 for the filter applied to heterogeneous regions. Fig. 4.b illustrates the case of setting $\beta=3.0$ which leads to even better edge/detail preservation but artifacts become more visible.

Fig. 5 shows the output images for two other adaptive versions. The output image obtained for DCT+Haar filter is presented in Fig. 5.a. An important feature is that many high-contrast small sized objects are preserved very well if they have been detected by the Level set method. The output for the combination of the DCT-based denoising and the filter introduced in [29] is shown in Fig. 5.b. The filter performed better noise suppression but edges and fine details are less sharp.

Table 6

Performance of the adaptive despeckling techniques

Combined filter description and parameters	Test image # 1			Test image # 2		
	MSE out	MSE het	MSSIM	MSE out	MSE het	MSSIM
DCT: 4.9 (comb) + 4.0 (hard frequency independent)	449	666	0.823	470	696	0.814
DCT 4.9 (comb) + 3.0 Haar wavelet (hard)	445	667	0.823	466	688	0.817
Adapt (DCT+Frost)	454	648	0.819	474	699	0.809
Adapt (DCT+Vozel 9)	429	617	0.825	457	654	0.814

Note that for all locally adaptive filters described here, the correspondence to the first or the second type of region is determined by the position of a block central pixel in edge map.

By visually checking the results, one can see that the filter preserved details in heterogeneous regions for simulated images. For this purpose, we applied the DCT based filter combined with frequency dependent thresholding with $\beta = 4.9$ for homogeneous regions and the DCT based filter with frequency independent threshold $T(m, n) = \beta \sigma_{\mu} I_{nm}^{med}$ for the detected

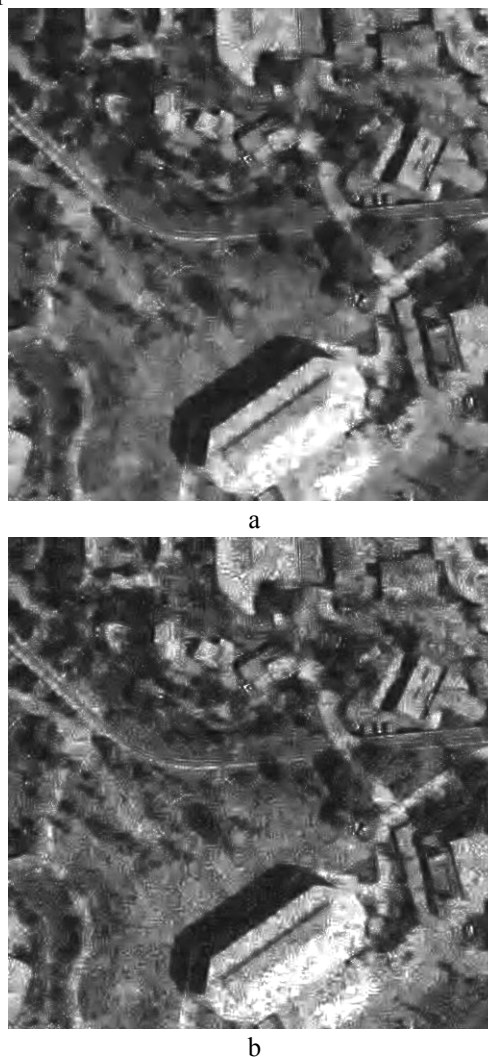


Fig. 4. Output images for DCT based adaptive filters with parameter switching in blocks depending upon edge (heterogeneity) map: a – $\beta = 4.0$, b – $\beta = 3.0$



Fig. 5. Output images for adaptive filters DCT+Haar (a) and DCT+integro-differential filter [29] (b)

Conclusions

A wide set of despeckling techniques is verified for two test images corrupted by spatially correlated speckle. It is shown that the main problem is to provide good edge/detail preservation. To solve this task, it is proposed to apply the Level Set method for detecting heterogeneities in SAR images and then to locally use filters that produce the best edge/detail preservation. Among the best methods to gain this purpose, we mention Haar wavelet filter adapted to multiplicative noise and the integro-differential method [29]. This is demonstrated by both quantitative data and some visual

examples. This work has been partly supported by French-Ukrainian program Dnipro (PHC DNIPRO 2013, PROJET N° 28370QL).

References

1. Oliver, C. *Understanding Synthetic Aperture Radar Images [Text]* / C. Oliver, S. Quegan. – SciTech Publishing, 2004. – 486 p.
2. *Fusion of high-resolution satellite SAR and optical images [Text]* / R. Chandrakanth, J. Saibaba, G. Varadan, P.A. Raj // *Proceedings of International Workshop on multi-platform/multi-sensor remote sensing and mapping*. – 2011. – P. 1-6.
3. Touzi, R. *A Review of Speckle Filtering in the Context of Estimation Theory [Text]* / R. Touzi // *IEEE Trans. on GRS*. – 2002. – Vol. 40, No 11. – P. 2392-2404.
4. *Locally Adaptive DCT Filtering for Signal-Dependent Noise Removal [Text]* / R. Oktem, K. Egiazarian, V. Lukin, N. Ponomarenko, O. Tsymbal // *EURASIP Journal on Advances in Signal Processing*, Article ID 42472. – 2007. – 10 p.
5. Solbo, S. *A stationary wavelet domain Wiener filter for correlated speckle [Text]* / S. Solbo, T. Eltoft // *IEEE Transactions on Geoscience and Remote Sensing*. – 2008. – Vol.46, No 8. – P. 1219–1230.
6. *Filtering of radar images based on blind evaluation of noise characteristics [Text]* / V.V. Lukin, N.N. Ponomarenko, S.K. Abramov, B. Vozel, K. Chehdi, J. Astola // *Proceedings of Image and Signal Processing for Remote Sensing XIV*. – 2008. – Vol. 7109. – 12 p.
7. Lee, J.-S. *Speckle analysis and smoothing of synthetic aperture radar images [Text]* / J.-S. Lee // *Comp. Vis. Graph. Im. Proc.* – 1981. – Vol. 17. – P. 24-32.
8. Naumenko, A.V. *Neural Network Based edge detection in Pre-filtered SAR Images [Text]* / A.V. Naumenko, V.V. Lukin, K.O. Egiazarian // *Proceedings of the 5-th World Congress "Aviation in the XXI-st Century"*. – 2012. – Vol. 2. – P. 3.7.61-3.7.66.
9. Medeiros, F.N.S. *Evaluation of speckle noise MAP filtering algorithms applied to SAR Images [Text]* / F.N.S. Medeiros, N.D.A. Mascarenhas, L.F. Costa // *Int. J. Remote Sensing*. – 2003. – Vol. 24, No 24. – P. 5197-5218.
10. *Improved Sigma Filter for Speckle Filtering of SAR Imagery [Text]* / J.-S. Lee, J.-H. Wen, T.L. Ainsworth, K-S. Chen, A.J. Chen // *IEEE Transactions on Geoscience and Remote Sensing*. – 2009. – Vol. 47, No 1. – P. 202-213.
11. Yun, S. *A new multiplicative denoising variational model based on m-th root transformation [Text]* / S. Yun, H. Woo // *IEEE Transactions on Image Processing*. – 2012. – Vol. 21, Issue 5. – P. 2523-2533.

12. A nonlocal SAR image denoising algorithm based on LLMMSE wavelet shrinkage [Text] / S. Parrilli, M. Poderico, C.V. Angelino, L. Verdoliva // *IEEE Transactions on Geoscience and Remote Sensing*. – 2012. – Vol. 50. Issue 2. – P. 606-616.
13. Denoising of single-look SAR images based on variance stabilization and non-local filters [Text] / M. Makitalo, A. Foi, D. Fevraleov and V. Lukin // *CD-ROM Proceedings of MMET*. – 2010. – 4 p.
14. Combining level Sets and Orthogonal Transform for Despeckling SAR Images [Text] / D.V. Fevraleov, S.S. Krivenko, V.V. Lukin, R. Marques, F. de Medeiros // *Авиационно-космическая техника и технология*. – 2013. – № 2/99. – С. 103-112.
15. Ponomarenko, N.N. Visually Lossless Compression of Synthetic Aperture Radar Images [Text] / N.N. Ponomarenko, V.V. Lukin, K.O. Egiazarian // *CD-ROM Proceedings of ICATT*. – 2011. – 3 p.
16. Dogan, O. Time Domain SAR Raw Data Simulation of Distributed Targets [Text] / O. Dogan, M. Kartal // *EURASIP Journal on Advances in Signal Processing*. – 2010. – 11 p.
17. Wang, Z. Multi-scale structural similarity for image quality assessment [Text] / Z. Wang, E.P. Simoncelli, A.C. Bovik // *IEEE Asilomar Conf. on Signals, Systems and Computers*. – 2003. – Vol. 2 – P. 1398-1402.
18. Novel Speckle Filter for SAR Images Based on Information-theoretic Heterogeneity Measurements [Text] / Z. Chen, J. Zhu, C Li., Y. Zhou // *Chinese Journal of Aeronautics (Elsevier Science Direct)*. – 2009. – Vol. 22. – P. 528-534.
19. Marques, R. Target Detection in SAR Images Based on a Level Set Approach [Text] / R.C.P. Marques, F.N.S. Medeiros, D.M. Ushizima // *IEEE Trans. on Systems, Man and Cybernetics*. – 2009. – Vol. 39, No 2. – P. 214-222.
20. Li, H. A Level Set Filter for Speckle Reduction in SAR Images [Text] / H. Li, B. Huang and X. Huang // *EURASIP Journal on Advances in Signal Processing*. – 2010. – 14 p.
21. Dibos, F. Image denoising through a level set approach [Text] / F. Dibos, G. Koepfler // *Proceedings of ICIP*. – 1998. – Vol. 3. – P. 264-268.
22. Sethian, J. Level Set Methods and Fast Margin Methods: Evolving Interfaces in Computational Geometry, Fluid Mechanics [Text] / J.A. Sethian. – *Comput. Vision and Materials Science, 1st ed.*; Cambridge University Press, 1998. – 420 p.
23. Marques, R. SAR image segmentation based on level set approach and GA0 model [Text] / R. Marques, F.N.S. Medeiros, J.S. Nobre // *IEEE Transactions on Pattern Analysis and Machine Intelligence*. – 2012. – Vol.34. – P. 2046-2057.
24. Performance evaluation for Blind Methods of Noise Characteristics Estimation for TerraSAR-X Images [Text] / V.V. Lukin, S.K. Abramov, D.V. Fevraleov, N.N. Ponomarenko, K.O. Egiazarian, J.T. Astola, B. Vozel, K. Chehdi // *Proceedings of SPIE/EUROPTO on Satellite Remote Sensing*. – 2011. – Vol. 8180. – 12 p.
25. Эффективность фильтрации одно-взглядовых PCA-изображений при пространственно-коррелированных помехах [Текст] / С.К. Абрамов, Р.А. Кожемякин, С.С. Кривенко, Н.Н. Пономаренко, В.В. Лукин // *Радиоелектронні і комп'ютерні системи*. – 2012. – № 3. – С. 18-25.
26. Color Image Database for Evaluation of Image Quality Metrics [Text] / N. Ponomarenko, M. Carli, V. Lukin, K. Egiazarian, J. Astola, F. Battisti // *Proceedings of International Workshop on Multimedia Signal Processing, Australia*. – 2008. – P. 403-408.
27. Lee, J. Digital image enhancement and noise filtering by use of local statistics [Text] / J. S. Lee // *IEEE Trans. Pattern Anal. Mach. Intell.* – 1980. – Vol. PAMI-2. – P. 165-168.
28. A model for radar images and its application to adaptive digital filtering of multiplicative noise [Text] / V.S. Frost, J. Stiles, K. Shanmugan, J. Holtzmann // *IEEE Trans. on PAMI*. – 1982. – Vol. 4. – P. 157-166.
29. Klaine, L. An integro-differential method for adaptive filtering of additive and multiplicative noise [Text] / L. Klaine, B. Vozel, K. Chehdi // *Proceedings of ICASSP*. – 2005. – Vol. 2. – P. 1001-1004.
30. Image denoising by sparse 3-D Transform-domain collaborative filtering [Text] / K. Dabov, A. Foi, V. Katkovnik, K. Egiazarian // *IEEE Transactions of Image Processing*. – 2007. – №8, Vol. 16. – P. 2080-2095.
31. Deledalle, C. Patch similarity under non Gaussian noise [Text] / C.A. Deledalle, F. Tupin // *Proceedings of ICIP*. – 2011. – 4 p.
32. Lukin, V. HVS-Metric-Based Performance Analysis Of Image Denoising Algorithms [Text] / V. Lukin, N. Ponomarenko, K. Egiazarian // *Proceedings of EUVIP*. – Paris, France. – 2011. – 6 p.
33. Pogrebnyak, O. Wiener DCT Based Image Filtering [Text] / O. Pogrebnyak, V. Lukin // *Journal of Electronic Imaging*. – 2012. – No 4. – 14 p.
34. Classification of Pre-filtered Multichannel Remote Sensing Images [Text] / V. Lukin, N. Ponomarenko, D. Fevraleov, B. Vozel, K. Chehdi, A. Kurekin // *Book Chapter in Remote Sensing I*. – 2012. – 24 p.
35. Efficiency analysis of color image filtering [Text] / D. Fevraleov, V. Lukin, N. Ponomarenko, S. Abramov, K. Egiazarian, J. Astola. *EURASIP Journal on Advances in Signal Processing*. – 2011. – Vol. 2011:41, doi:10.1186/1687-6180-2011-41. – 2011. – 19 p.

Поступила в редакцию: 24.09.2013, рассмотрена на редколлегии 25.09.2013

Рецензент: д-р техн. наук, проф., проф. каф. «Проектирование радиоэлектронных систем летательных аппаратов» В.К. Волосюк, Национальный аэрокосмический университет им. Н.Е. Жуковского "ХАИ", г. Харьков.

АНАЛИЗ ЭФФЕКТИВНОСТИ КОМБИНИРОВАННОГО ПОДАВЛЕНИЯ СПЕКЛА В ОДНОВЗГЛЯДОВЫХ РСА-ИЗОБРАЖЕНИЯХ

Р.А. Кожемякин, С.С. Кривенко, В.В. Лукин, Р. Маркес, Ф. Медейрос, Б. Возель

В данной статье проводится оценка эффективности фильтрации спекла для изображений, формируемых радиолокаторами с синтезированной апертурой (РСА), с помощью модели данных, которая учитывает основные свойства реальных однозглядовых изображений, в частности, негауссову функцию плотности вероятности спекла и его пространственную корреляцию. Анализ проводится для широкого множества хорошо известных методов фильтрации спекла, а также для недавно предложенных локально-адаптивных фильтров, сочетающих метод уровней множеств, использующийся для обнаружения малогабаритных объектов, и дискретное косинусное преобразование. Результаты оцениваются при помощи стандартного критерия MSE, локального MSE, рассчитываемого на неоднородных участках, и интегрального показателя MSSIM. Результаты показали, что локально-адаптивная фильтрация по ряду параметров превосходит все известные методы фильтрации.

Ключевые слова: однозглядовое РСА изображение; комбинированная фильтрация спекла; метод уровней множеств, ДКП, анализ эффективности.

АНАЛІЗ ЕФЕКТИВНОСТІ КОМБІНОВАНОГО ПРИДУШЕННЯ СПЕКЛА В ОДНОПОГЛЯДОВИХ РСА-ЗОБРАЖЕННЯХ

Р.О. Кожемякін, С.С. Кривенко, В.В. Лукін, Р. Маркес, Ф. Медейрос, Б. Возель

У даній статті проведено оцінку ефективності фільтрації спекла для зображень, що сформовані радіолокаторами із синтезованою апертурою (РСА), за допомогою моделі даних, яка враховує основні властивості реальних однопоглядових зображень, зокрема, негаусову функцію щільності ймовірності спекла та його просторову кореляцію. Аналіз проводиться для найбільш відомих методів фільтрації спекла, а також для нещодавно запропонованих локально-адаптивних фільтрів, що поєднують метод рівневих множин, що використовується для виявлення малогабаритних об'єктів, та дискретне косинусне перетворення. Результати оцінюються за допомогою стандартного критерію MSE, локального MSE, що розраховується на неоднорідних ділянках, і інтегрального показника MSSIM. Результати показали, що локально-адаптивна фільтрація по ряду параметрів перевершує всі відомі методи фільтрації.

Ключові слова: однопоглядове РСА зображення; комбінована фільтрація спекла; метод рівневих множин, ДКП, аналіз ефективності.

Кожемякин Руслан Александрович – аспирант каф. «Приема, передачи и обработки сигналов», Национальный аэрокосмический университет им. Н.Е. Жуковского «ХАИ», г. Харьков, Украина, e-mail: lukin@ai.kharkov.com.

Кривенко Сергей Станиславович – канд. техн. наук, с.н.с. каф. «Приема, передачи и обработки сигналов», Национальный аэрокосмический университет им. Н.Е. Жуковского «ХАИ», г. Харьков, Украина, e-mail: krivenkos@inbox.ru.

Лукин Владимир Васильевич – д-р техн. наук, проф., проф. каф. «Приема, передачи и обработки сигналов», Национальный аэрокосмический университет им. Н.Е. Жуковского «ХАИ», г. Харьков, Украина, e-mail: lukin@ai.kharkov.com.

Регис Маркес – аспирант, Федеральный университет штата Сеара, Форталеза, Бразилия, e-mail: prof.regismarques@gmail.com.

Фатима Сомбра де Медейрос – доктор наук в области физики, профессор, Федеральный университет штата Сеара, Форталеза, Бразилия, e-mail: fsombraufc@gmail.com.

Возель Бенуа – профессор, университет Ренн, Ланьон, Франция, e-mail: benoit.vozel@univ-rennes1.fr.